PROCEEDINGS OF SCIENCE

Measurement of the cosmic ray (e^++e^-) flux with AMS

Valerio Vagelli[*†]
INFN Sezione di Perugia, I-06100 Perugia, Italy
E-mail: valerio.vagelli@pg.infn.it

The cosmic ray ($e^+ + e^-$) flux has been measured by the Alpha Magnetic Spectrometer (AMS-02) in the energy range 0.5 GeV to 1 TeV, based on the analysis of 10.6 million $e^\pm$ events collected during the first 30 months of data taking. The statistics and the resolution of the AMS-02 detector provide an accurate measurement in the whole energy range. No features have been observed in the flux, and the ($e^+ + e^-$) spectrum can be accurately described by a single power law above 30 GeV. The procedures and the data analysis techniques for the ($e^+ + e^-$) flux measurement are reviewed in this report.

The European Physical Society Conference on High Energy Physics
22-29 July 2015
Vienna, Austria

[*]Speaker.
[†]On behalf of the AMS collaboration

PoS(EPS-HEP2015)613

The measurement of electrons and positrons ($e^{\pm}$) in cosmic rays (CRs) provides fundamental information about their origin and propagation in the Galaxy. CR $e^{\pm}$ amount to only $\sim$1% of the total CR flux measured at Earth. Nonetheless, the experimental efforts faced to measure the features of the $e^{\pm}$ fluxes have been dynamic and diverse in the last 50 years: CR $e^{\pm}$ can in fact probe the models of CR origin and propagation in an independent and complementary approach with respect to that of the more abundant hadronic CR component. Being the lightest charged CR species, they experience peculiar and different energy losses. Moreover, their spectral features above $\sim$ 10 GeV may be sensitive to additional CR sources currently not taken into account in the current models, like Dark Matter annihilation or production in nearby pulsars, or to unconventional acceleration and propagation mechanisms [1]. Recently, measurements of the positron fraction $e^+/(e^+ + e^-)$ and of the e^+ flux up to 500 GeV, and of the e^- flux up to 700 GeV by the Alpha Magnetic Spectrometer (AMS-02) [2, 3] have confirmed the existence of an additional $e^{\pm}$ source at high energies beyond well established astrophysical mechanisms. The AMS measurements of e^+ and e^- fluxes are discussed in [4]. This contribution reviews the AMS measurement of the CR $(e^+ + e^-)$ flux from 0.5 GeV to 1 TeV, based on the analysis presented in details in [5].

1. The AMS-02 detector

AMS-02 is a general purpose high-energy particle physics detector which has been installed on the International Space Station in May 2011 to conduct a long-duration ($\sim$20-year) mission for the accurate measurement of CR composition and energy spectra up to the TeV scale. The AMS-02 detector is fully described in [6]. Figure 1 shows the AMS-02 detector and the response of its subdetectors for different species of CRs.

The core of AMS-02 consists of 9 planes of double sided silicon microstrip tracker and a 0.14 T permanent magnet. The measurement of the energy losses in the tracker planes are used to determine the particle charge, Z. The plane crossing coordinates determine the particle trajectory and curvature in the magnetic field. The curvature yields the particle charge sign used to separate matter and antimatter CRs. The particle rigidity $R = p/Z$, where p is the momentum, is measured over a lever arm up to 3 m. The maximum detectable rigidity for $|Z| = 1$ particles is 2 TV.

Four time of flight (TOF) planes trigger the readout of the detector and measure the particle velocity and flight direction. An anti-coincidence veto system located inside the magnet bore rejects particles outside the acceptance of the detector with inefficiency lower than 10^{-5}.

To improve the particle identification capabilities, AMS-02 is equipped with a transition radiation detector (TRD), a ring imaging Cherenkov detector and an electromagnetic calorimeter (ECAL) .

The 3-dimensional imaging capability of the 17 radiation length ($17X_0$) ECAL provides the accurate measurement of the $e^{\pm}$ energy scaled to the top of AMS-02 (E). The topology of the shower reconstructed in ECAL is exploited to separate $e^{\pm}$ from hadrons.

The energy deposit in the 20 layers of proportional tubes in the TRD are exploited to further differentiate between $e^{\pm}$ and protons. The magnet, located between TRD and ECAL, ensures that the information provided by the two subdetectors are independent from each other.

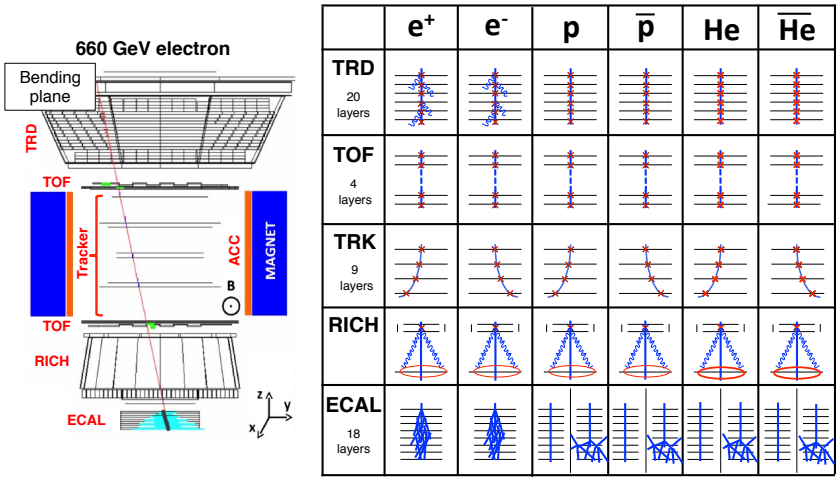

Figure 1: Left – Event display of a 660 GeV e^- crossing AMS-02. Right – Response of the AMS-02 subdetectors for different matter/antimatter CRs. The redundant identification capabilities of AMS-02 allow to precisely measure the particle properties and to distinguish different species of CRs.

2. Data analysis

The result presented in this contribution is based on the analysis of the $\sim 41 \times 10^9$ events collected by AMS-02 in the first 30 months of data taking. The data have been analyzed to measure the isotropic $\Phi(e^+ + e^-)$ flux, which for each energy bin of width ΔE is defined as:

$$\Phi(e^+ + e^-) = \frac{N(E)}{A(E) \cdot \varepsilon_T(E) \cdot \varepsilon_E(E) \cdot T(E) \cdot \Delta E} \tag{2.1}$$

where A is the effective detector acceptance, ε_T is the trigger efficiency, ε_E is the ECAL signal selection efficiency and T is the exposure time; N is the number of events identified as $e^\pm$, after the rejection of secondary particles of atmospheric origin [7].

The measurement of $\Phi(e^+ + e^-)$ has been performed in 74 independent energy intervals (bins) from 0.5 GeV to 1 TeV. The effects introduced by the event bin-to-bin migration due to the finite ECAL resolution have been measured to be negligible with respect to other systematic uncertainties discussed below. The calorimeter energy scale has been calibrated during a test beam at CERN with $e^\pm$ beams from 10 GeV/c to 290 GeV/c. In space, the energy scale is constantly monitored by using minimum ionizing particles and by the comparison of the energy measurement E with the tracker momentum measurement p for $e^\pm$ and protons. The ECAL energy scale is known with a precision of 2% in the test beam energy range. The uncertainty increases up to 5% at 0.5 GeV and at 1 TeV.

A selection based on the TRD, tracker and TOF subdetectors has been applied to identify downward-going relativistic $|Z|$=1 particles in the TRD and ECAL acceptance. Such sample contains the $e^\pm$ signal and the dominating proton background. Protons interacting deep in the calorimeter have been efficiently removed by rejecting particles that only ionize in the first $5\,X_0$ of the ECAL. The sample purity has been further enhanced by a selection based on the ECAL shower topology.

A data-driven approach has been exploited to evaluate the amount of $(e^+ + e^-)$ in the signal enriched sample. The signals from the 20 TRD layers have been combined into a single discriminating variable, the *TRD classifier*, derived from the product of the probabilities of the $e^\pm$ hypothesis.

A standard template-fit procedure on the TRD classifier shapes has been applied, independently in each energy bin, to measure the yield of $(e^+ + e^-)$ events, N, and the statistical uncertainty on N and on the number of background events. Figure 2 shows the TRD classifier reference shapes and an example of template-fit. A total of 10.6×10^6 $(e^+ + e^-)$ events have been identified from 0.5 GeV to 1 TeV. The statistical fluctuations on N dominate the measurement uncertainty above ∼200 GeV.

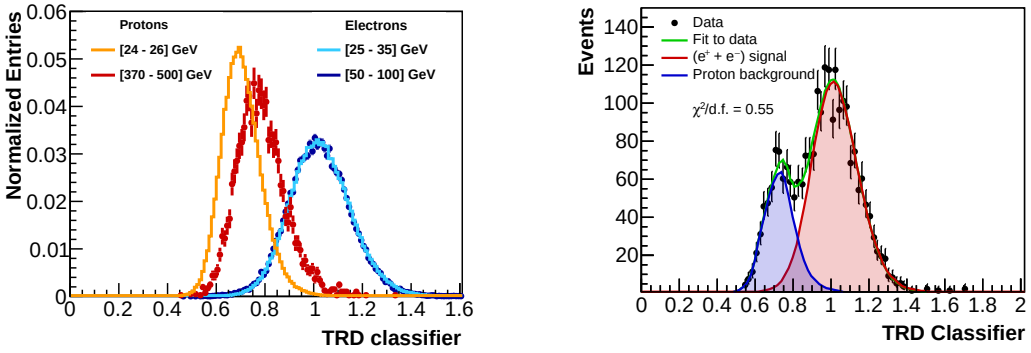

Figure 2: Left – TRD classifier reference shapes for $e^\pm$ (blue and light blue) and protons (red and orange) in different energy ranges. The TRD classifier distribution does not depend on the energy for $e^\pm$ above 10 GeV. Right – Template-fit to the [149-170] GeV energy bin used to extract the yield of $(e^+ + e^-)$ events.

The templates for the $e^\pm$ signal and for the proton background have been retrieved from the data, separately in each bin, using pure samples of e^- and protons selected with ECAL. The signal template does not show any energy dependence above ∼10 GeV. Therefore, all the e^- selected with high purity in the [15.1, 83.4] GeV energy range have been used to define a unique, well known, *universal* signal template used up to the highest energies.

The systematic uncertainty on $N_E = N/\varepsilon_E$ is defined by the level of accuracy to which the data driven template shapes and ε_E are known. To evaluate this, the complete analysis has been performed 2000 times in each energy bin, for different levels of background contaminations and different ECAL selections used to define the TRD classifier templates (see Figure 3, Left). The stability of the result for all the trials quantifies the systematic uncertainty of N_E, which amounts to <1% below ∼200 GeV and it increases to 4% in the 500–700 GeV bin. Above ∼500 GeV, it represents the dominating source of systematic uncertainty for the $\Phi(e^+ + e^-)$ measurement.

The acceptance for $e^\pm$ passing through the AMS-02 active volumes has been evaluated using a Monte Carlo (MC) simulation of the AMS-02 detector based on the Geant 4.9.4 package [8]. The geometric acceptance for $e^\pm$ amounts to ∼550 cm^2 sr. The event selection efficiency amounts to 90% at 10 GeV and decreases up to 70% at 1 TeV. The effective acceptance A has been corrected by the tiny differences observed between the data and the MC simulation, shown in Figure 3 (Right) for the case of the TRD selection. The uncertainty on the correction, which amounts to 2% above 3 GeV and which introduces a bin-to-bin correlation of 1.4% over the entire energy range, dominates the measurement systematic uncertainty below ∼500 GeV.

The trigger efficiency, ε_T, has been determined from data using a dedicated, unbiased trigger stream. It amounts to 100% above 3 GeV and decreases down to 75% at 1 GeV.

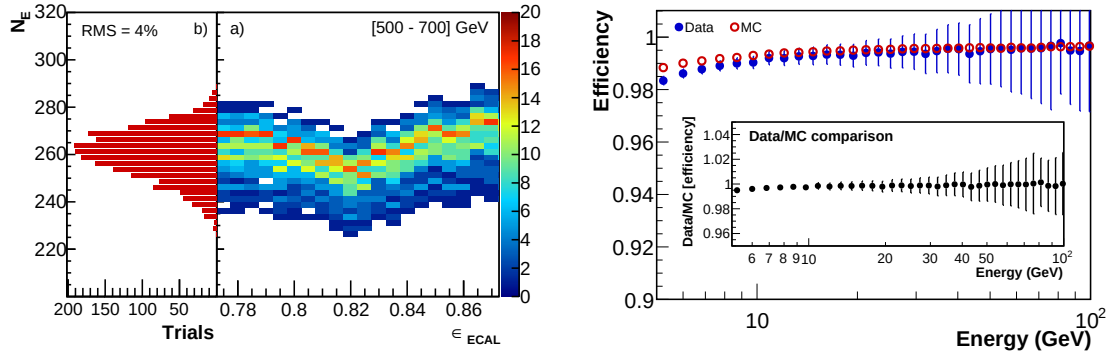

Figure 3: Left – Procedure to assess the systematic uncertainty on N_E, quantified by the spread of the results for different analysis trials (b). Insert (a) shows the stability of N_E for different strengths of the ECAL selection, therefore for different amounts of proton background contaminations. Right – Data / MC simulation comparison for the selection on the TRD reconstruction and quality. The efficiency ratio – evaluated for each analysis selection and shown in the insert for the TRD selection only – provides the correction to apply to the effective acceptance A retrieved from the MC simulation.

The exposure time T has been calculated, independently in each energy bin, by the sum of livetime-weighted seconds of data taking. It amounts to 6.2×10^7 s above 30 GeV and it decreases below 30 GeV due to the non-negligible effect of the geomagnetic cutoff.

3. Result

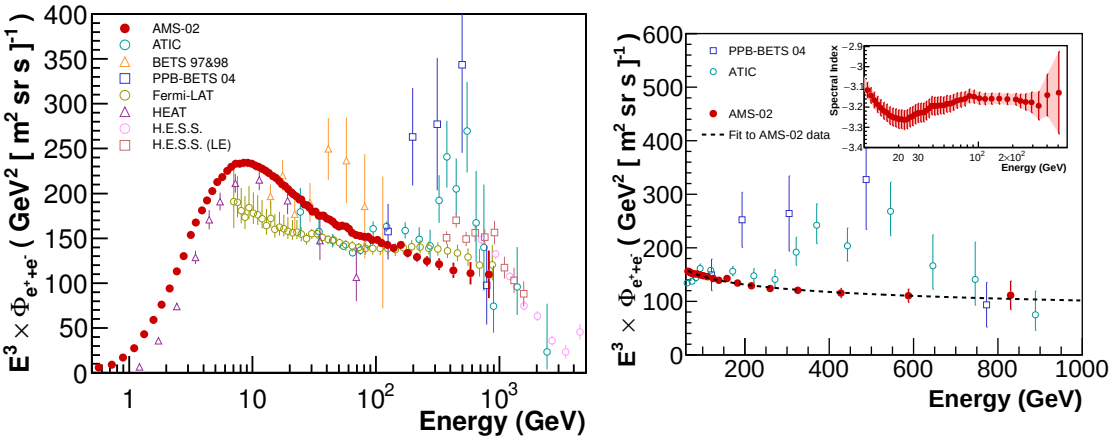

Figure 4: Left – AMS-02 measurement of $\Phi(e^+ + e^-)$ (red points) superimposed to previous measurements[9, 10, 11, 12, 13, 14, 15]. Right – Single power law fit ($\Phi \propto E^{-|\gamma|}$) to the AMS-02 data (black line). The detailed measurement of the energy dependence of the local spectral index (γ) is shown in the insert.

The AMS $\Phi(e^+ + e^-)$ measurement – evaluated using Equation 2.1 – is reported in Figure 4 (Left) together with previous measurements. The data show no relevant feature and the flux is

smooth above 10 GeV. Below this energy, $\Phi(\mathrm{e}^+ + \mathrm{e}^-)$ is modulated by the effect of the Solar Wind.

As shown in Figure 4 (Right), the existence of a prominent spectral feature above 300 GeV observed by previous experiments is excluded. Other possible spectral anomalies are strongly constrained. The flux measured by AMS-02 results softer than previous measurements at high energies. Within the current experimental accuracy, the $(\mathrm{e}^+ + \mathrm{e}^-)$ flux can be described by a single power law ($\Phi \propto E^{-|\gamma|}$) above 30 GeV, with $\gamma = -3.170 \pm 0.008$ (stat+syst) ± 0.008 (energy scale) . More details about the analysis of the energy dependence of $\Phi(\mathrm{e}^+ + \mathrm{e}^-)$ are discussed in [5].

The measurement discussed here is based on the analysis of the data collected by AMS-02 in its first 30 months of operations. This corresponds to $\sim 15\%$ of the expected data sample for the whole AMS mission. The analysis of additional data collected by AMS-02 in the future years will provide further advances in the measurement accuracy and energy reach, that will improve the current knowledge of the features of CR $\mathrm{e}^{\pm}$ towards a comprehensive understanding of their origin, acceleration and propagation mechanisms.

Acknowledgments

This work has been supported by persons and institutions acknowledged in [5].

References

[1] L. Feng et al., *Phys. Lett.* **B 728** (2014) 250;
K. Blum et al., *Phys. Rev. Lett.* **111** (2013) 211101;
L. Bergström et al., *Phys. Rev. Lett.* **111** (2013) 171101;
I. Cholis and D. Hooper, *Phys. Rev.* **D 88** (2013) 023013;
T. Linden and S. Profumo, *Astrophys. J.* **772** (2013) 18.

[2] L. Accardo et al., *Phys. Rev. Lett.* **113** (2014) 121101.

[3] M. Aguilar et al., *Phys. Rev. Lett.* **113** (2014) 121101.

[4] N. Zimmermann, in proceedings of *EPS-HEP 2015*, PoS(EPS-HEP2015)400.

[5] M. Aguilar et al., *Phys. Rev. Lett.* **113** (2014) 221102.

[6] M. Aguilar et al., *Phys. Rev. Lett.* **110** (2013) 141102.

[7] D. Smart and M. Shea, *Adv. Sp. Res.* **36** (2005) 2012;
C. Størmer, *Q. J. R. Meteorol. Soc.* **82** (1956) 115.

[8] J. Allison et al., *IEEE Trans. Nucl. Sci.* **53** (2006) 270;
S. Agostinelli et al., *Nucl. Instr. Meth.* **A 506** (2003) 250.

[9] S. Torii et al., *Astrophys. J.* **559** (2001), 973.

[10] M. A. DuVernois et al., *Astrophys. J.* **559** (2001) 296.

[11] J. Chang et al., *Nature* (London) **456** (2008) 362.

[12] K. Yoshida et al., *Adv. Sp. Res.* **42** (2008) 1670.

[13] F. Aharonian et al., *Phys. Rev. Lett.* **101** (2008) 261104.

[14] F. Aharonian et al., *Astron. Astrophys.* **508** (2009) 561.

[15] M. Ackermann et al., *Phys. Rev.* **D82** (2010) 092004.